CATALYSIS IN OIL
REFINING INDUSTRY

Physicochemical and Catalytic Properties of Bifunctional Catalysts with Different Contents of Zeolite ZSM-22 in the Hydrodeoxygenation of Sunflower Oil

A. A. Nepomnyashchii[a, *, **], **E. R. Saibulina**[a], **E. A. Buluchevskiy**[a], **T. I. Gulyaeva**[a],
R. M. Mironenko[a], **O. V. Potapenko**[a], **and A. V. Lavrenov**[a]

[a] Center of New Chemical Technologies, Boreskov Institute of Catalysis,
Siberian Branch, Russian Academy of Sciences, Omsk, 644040 Russia
*e-mail: himik@ihcp.ru
**e-mail: workbox_555@mail.ru

Abstract—The authors study the effect of the content of zeolite ZSM-22 (15−70 wt %) in a support on the physicochemical properties of Pt/ZSM-22−Al_2O_3 catalysts. The dependence of the yield and composition of sunflower oil hydrodeoxygenation products on these catalysts on the temperature (310−340°C), pressure (3−5 MPa), and weight hourly space velocity (WHSV) (0.8−3 h^{-1}) is determined. The possibility is shown of the full hydrodeoxygenation of sunflower oil with the formation of C_{5+} hydrocarbons containing up to 72% of *iso*-paraffins with yields of 75−79 wt %.

INTRODUCTION

Inedible and waste vegetable oils and animal fats are considered alternative feedstocks for the production of motor fuels [1]. Despite the attractiveness of first-generation biofuel (fatty acid methyl esters), its high viscosity and pour temperature with low heat of combustion and stability due to a high content of oxygen stimulate the search for other ways of processing renewable biomass [2]. One trend is the catalytic hydroprocessing of oil−fat feedstocks when the product is a mixture rich in C_8−C_{24} *iso*- and *n*-alkanes with high cetane numbers and low cloud and filtration temperatures [3].

Industrial catalytic hydroprocessing has two stages: hydrodeoxygenation and hydrodewaxing. The first stage is the hydrogenation and deoxygenation of fatty acid triglycerides to saturated C_{15}−C_{18} hydrocarbons using such traditional hydrotreatment catalysts as sulfide Ni-Mo/Al_2O_3, Co-Mo/Al_2O_3, and Ni-W/Al_2O_3 [4, 5]. The high content of *n*-alkanes in products of hydrotreatment on these catalysts requires further dewaxing on Pt/zeolite catalysts to improve their low-temperature properties [6, 7]. There have also been attempts to perform the single-stage processing of vegetable oils on one catalyst. Bifunctional catalysts with nickel or a noble metal (Pt, Pd) on zeolite supports with a one-dimensional 1D-10R structure of channels (SAPO-11 [8, 9], ZSM-22 [10, 11], ZSM-23 [11]) were used for this purpose. Studies the *n*-alkane isomerization mechanism with zeolite ZSM-22 have established that the reaction generally occurs on acid sites in pore throats, and its products are predominantly multimethyl substituted isomers. The use of zeolites with 1D-10R channels also allows us to reduce the rate of coking and lengthen the lifetime of the catalysts. The acidity and structural features of their porous structure also allow such zeolites to be used in the isodewaxing of diesel and oil fractions [12−14].

The authors [10, 11] proposed using nickel and platinum catalysts with 70 : 30 mixtures of ZSM-22−Al_2O_3 as supports for the single-stage processing of soybean oil. However, no high yield of liquid products could be ensured on these catalysts to reach 50−55% conversion (though the content of *iso*-alkanes in them was as high as 91%), due to an increased contribution from cracking reactions. Such results could have been caused by excessive catalyst acidity due to using less than optimal zeolite/Al_2O_3 in the supports and high process temperatures (357−370°C).

This aim of this paper was to studying the effect of the content of zeolite ZSM-22 in a platinum catalyst support and the temperature, pressure, and feedstock hourly space velocity on the composition and yield of sunflower oil single-stage hydroprocessing products.

EXPERIMENTAL

Preparation of Supports and Catalysts

The catalysts were prepared from boehmite of industrial production (AO Promkataliz) with a humidity of 78 wt %, commercial zeolite ZSM-22 with a module of 90 and a Na_2O content of 0.015 wt % (Zeolyst International), and $H_2PtCl_6 \cdot 6H_2O$ (≥99.99%, AO Krastsvetmet).

Zeolite powder was mixed with a suspension of boehmite used as a binding material with subsequent evaporation to a plastic mass, from which (5−7) × 2 mm extrudates were formed. The resulting extrudates were allowed to stand in air for 10−12 h at room temperature, dried for 10−12 h at 120°C, and calcined for 4 h at 550°C. The content of zeolite in the support was varied from 15 to 70 wt %.

The catalysts were prepared via the incipient wetness impregnation of supports (0.2−0.5 mm) with an aqueous H_2PtCl_6 solution, followed by drying for 12 h at 120°C and calcined for 4 h at 450°C. The calculated content of platinum in the catalysts was 1 wt %. Here and below, the catalyst samples are denoted as Pt/Z(x), where x is the ZSM-22 content in the support (wt %).

Characterization of Supports and Catalysts

The contents of sodium, aluminum, silicon, and platinum in the zeolites and catalysts was determined via atomic absorption spectrometry (AAS) on a Shimadzu AA-6300 spectrometer (Japan) and inductively coupled plasma atomic emission spectrometry on a Varian 710-ES spectrometer (United States). Samples were prepared by dissolving them in mineral acids (H_2SO_4, $HClO_4$, HF).

The phase composition of samples was studied via X-ray diffraction on a Bruker D8 Advance powder diffractometer with monochromatic CuK_α radiation ($\lambda = 1.5406$ Å) and a Lynxeye position-sensitive detector. The samples were scanned at room temperature in the 4° to 70° range of 2θ angles with a scanning step of 0.05° at an accumulation time of 2 s per point, a voltage of 40 kV, and a heating current of 40 mA. The recorded X-ray diffraction patterns were decoded using the ICDD powder X-ray diffraction database PDF-2 (2006).

The textural characteristics of zeolite and catalysts were studied via low-temperature nitrogen adsorption on a Micromeritics ASAP 2020 static volumetric vacuum analyzer at a temperature of −195.7°C in the 10^{-5} to 0.996 range of relative equilibrium pressures p/p_0. Prior to adsorption measurements, the samples were thermoevacuated for 10 h at 300°C. The specific surface area (S_{BET}) was calculated according to the Brunauer−Emmett−Teller (BET) procedure at p/p_0 ranging from 0.01 to 0.10. The total pore volume (V_{pore}) was determined from nitrogen adsorption at an equilibrium relative pressure of 0.990, assuming that the absorbate density was the same ad for a normal liquid (0.808 g/cm^3). The specific outer surface area (S_{out}), determined for zeolite as the sum of surface areas for meso- and macropores, and the volume of micropores (V_μ) were estimated using the comparative t-approach.

The acidity of zeolite and catalysts was estimated via ammonia temperature-programmed desorption (TPD) on a Micromeritics AutoChem 2920 analyzer equipped with a thermal conductivity detector. TPD profiles were measured in the 100−550°C range of temperatures at a measuring cell heating rate of 10°C/min. The helium flow rate through the reactor was 30 mL/min. Prior to experiment, the samples were purged in a helium flow for 1 h at a temperature of 550°C and then cooled to 100°C with subsequent ammonia adsorption at the same temperature.

Temperature-programmed reduction (TPR) was performed on a Micromeritics AutoChem II 2920 chemosorption analyzer in the temperature range of 35−500°C at a heating rate of 10°C/min for the measuring cell with the sample using a 10 vol % H_2−Ar calibration mixture. The flow rate through the reactor with the sample was 30 cm^3/min. The dispersity of metals was determined through the pulsed chemosorption of CO. Chemosorption was performed after TPR and cooling the sample in an inert gas flow to room temperature. A 10 vol % CO−He mixture was injected by pulses into the flow of an inert carrier gas in equal time intervals. Stoichiometry CO : Pt = 1 : 1 was used in calculating the dispersity of Pt.

Catalysts Testing and Product Analysis

The catalysts were tested for 8 h on a laboratory flow setup with a fixed catalyst bed at a hydrogen pressure of 3−5 MPa, a temperature of 310−340°C, a weight hourly space velocity (WHSV) of 0.8−3 h^{-1}, and a H_2 : feedstock ratio of 2500 Nm^3/m^3. A catalyst sample (1.8−7.0 g) was loaded into a U-shaped steel reactor and reduced for 1 h in a H_2 flow at 500°C. The reactor was then cooled to the temperature of the reaction to supply the feedstock. Refined sunflower oil (Yug Rusi Group, Aksai, Rostov oblast, Russia), whose fatty acid composition was given in [15], was used as a feedstock. The experimental conditions were selected (using catalyst particles 0.2−0.5 mm in size) so there would be no diffusion limitations in the process of the catalytic experiment.

Liquid and gaseous products were separated at atmospheric pressure and temperatures of 10−50°C. The composition of gaseous products was determined in real time using a Chromos GC-1000 dual-channel gas chromatograph. The inorganic components of the gas phase (H_2, CO, CO_2, and H_2O) were analyzed on two packed columns (length, 3 m; diameter, 4 mm) filled with sorbent Porapak R and activated charcoal

and equipped with a thermal conductivity detector. The hydrocarbon components of the gas phase (C_1–C_4, C_{5+}) were analyzed on a capillary column (J&W DB-1; length, 60 m; inner diameter, 0.25 mm; phase thickness, 1.00 μm) equipped with a flame ionization detector.

The qualitative composition of the stable liquid product was studied via gas chromatography/mass spectrometry (GC/MS) on an Agilent Technologies 6890/5973N complex with an HP 6890N gas chromatograph and an MCD5973N mass selective detector. A capillary column (HP-5MS; length, 30 m; inner diameter, 0.25 mm; phase thickness, 0.25 μm) was used for chromatographic separation under temperature-programmed conditions. Results were processed with the MSD Chem Station and NIST-05 MS Search 05 software (library of mass spectra and structural formulas). To estimate the completeness of oxygen removal and the group composition, the liquid hydrocarbon product was also analyzed via ^1H and ^{13}C NMR on a Bruker Avance-400 spectrometer at working frequencies of 400 (^1H) and 101 (^{13}C) MHz. $CDCl_3$ was used as the solvent.

The quantitative composition of liquid product samples was determined via gas-liquid chromatography on a Chromos GC-1000 gas chromatograph equipped with a capillary column (Restek Rtx-1; length, 105 m; inner diameter, 0.25 mm; phase thickness, 0.50 μm) and a flame ionization detector.

RESULTS AND DISCUSSION

Composition and Physicochemical Characteristics of Supports and Catalysts

The X-ray diffraction pattern of commercial zeolite ZSM-22 (Fig. 1) was in good agreement with the reference X-ray diffraction pattern (PDF no. 00-044-1390) indicating that the sample had high degrees of crystallinity and phase purity [12, 16]. The phase composition of 1% Pt/Z(x) catalysts was characterized by two phases: zeolite and a crystalline γ-Al_2O_3 binder (see Fig. 1). No reflections from platinum were
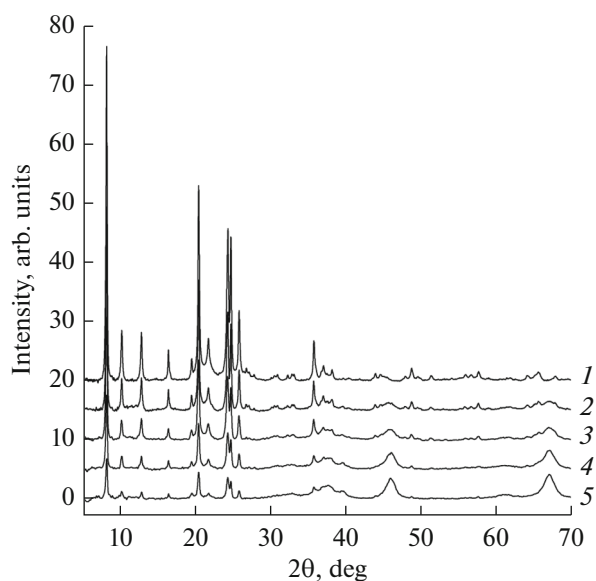
Fig. 1. X-ray diffraction patterns of (*1*) ZSM-22 zeolite and (*2*) 1% Pt/Z(70), (*3*) 1% Pt/Z(50), (*4*) 1% Pt/Z(30), and (*5*) 1% Pt/Z(15) catalysts.

revealed in the X-ray diffraction pattern likely due to its low content and high dispersity.

We can see from the data in Table 1 that the textures of the studied catalysts were determined by additive contributions from the pores of the initial materials, aluminum oxide and zeolite. The specific surface areas of all the studied catalysts were 189–213 m^2/g. When the content of zeolite in the supports was increased, a natural drop in the volume of mesopores was observed alongside a rise in the volume of micropores, the percentage of which reached 20% in the sample with 70 wt % of zeolite in the support.

The total desorption of ammonia for all the studied samples was 600–660 μmol/g. The ammonia TPD profiles for initial aluminum oxide and ZSM-22 contained a low-temperature desorption peak at 173°C indicating that the samples contained weak acid sites. In the region of higher temperatures, aluminum oxide was characterized by a flat peak with a maximum at

Table 1. Textural characteristics and CO chemosorption data for catalysts 1% Pt/Z(x)

Sample	C_{Pt}, wt %*	S_{BET}, m^2/g	V_{pore}, cm^3/g	V_{meso}, cm^3/g	V_μ, cm^3/g	D, %**
1% Pt/Al_2O_3	1.00	207	0.390	0.390	—	84
1% Pt/Z(15)	0.94	189	0.360	0.357	0.003	55
1% Pt/Z(30)	0.97	200	0.340	0.328	0.012	45
1% Pt/Z(50)	0.98	205	0.280	0.249	0.031	46
1% Pt/Z(70)	0.99	213	0.240	0.193	0.047	44
ZSM-22	—	247	0.180	0.097	0.083	—

 * Content of platinum in the catalysts, according to AAS data.
** Dispersity of platinum, according to CO chemosorption data.
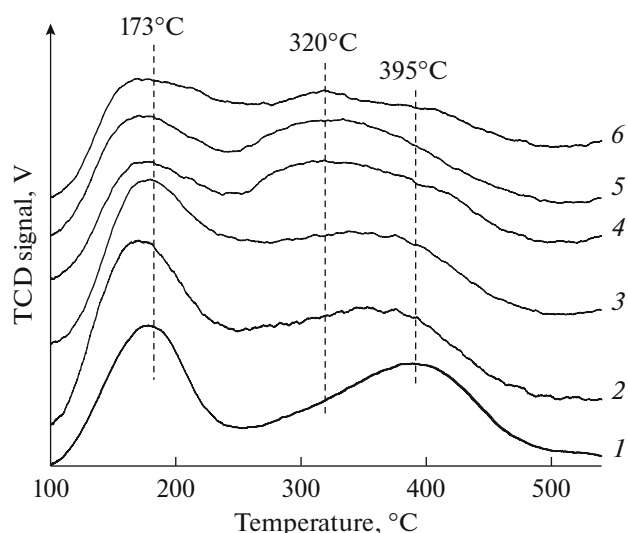
Fig. 2. TPD NH$_3$ profiles of (*1*) initial ZSM-22 zeolite and (*2*) 1% Pt/Z(15), (*3*) 1% Pt/Z(30), (*4*) 1% Pt/Z(50), (*5*) 1% Pt/Z(70), and (*6*) 1% Pt/A catalysts.

≈320°C, indicating the existence of medium-strength sites and, apparently, some strong acid sites. The desorption curve of zeolite had a sharp peak with a maximum at 395°C, which corresponds to the desorption of ammonia from strong acid sites. The TPD profiles of the catalysts on mixed supports were of similar character, and their acidic properties were generally determined by the acidity of initial materials.

The TPD profiles of all the catalysts (Fig. 3) had a region of hydrogen adsorption in the 150−250°C range of temperatures, corresponding to the reduction of PtO$_x$ particles to Pt^0. For the samples with high contents zeolite (50 and 70 wt %), the maximum in this region of hydrogen adsorption was shifted toward lower temperatures (175°C), indicating that the process of PtO$_x$ reduction is simpler than in catalysts with 15 and 30 wt % of zeolite. The high-temperature hydrogen adsorption peak in the TPR profiles (a maximum at 328 or 340°C) and the growth of its intensity when the content of zeolite in Pt/Z(x) catalysts was increased could indicate the presence of large, poorly reducible platinum particles, and strong interaction between the metal and the support [18].

According to data from pulsed CO chemosorption, the catalyst with a zeolite content of 15 wt % had the greatest dispersity of platinum (55%) (see Table 1). Raising the content of zeolite has a slight effect on the dispersity of platinum in the synthesized samples [19]. The values of platinum dispersity in the catalysts with 30 to 70 wt % of zeolite were close at 44−46%.

Hydrodeoxygenation of Sunflower Oil on 1% Pt/Z(x) Catalysts

Effect of the Content of Zeolite

All 1% Pt/Z(x) catalysts exhibit high activity in the sunflower oil conversion reactions and guarantee its complete conversion at a temperature of 320°C, a pressure of 4 MPa, and an WHSV of 1 h^{-1}. According to GC/MS and NMR spectroscopy data, the liquid products obtained in 8 h of experiment mainly contain aliphatic C$_{5+}$ hydrocarbons. No oxygen-containing compounds have been revealed. Products of gaseous sunflower oil hydrodeoxygenation are C$_1$−C$_4$ hydrocarbons, CO, CO$_2$, and H$_2$O.

Sunflower oil generally contains triglycerides of unsaturated C$_{16}$ and C$_{18}$ fatty acids. Assuming that oxygen is removed only in the form of water, the theoretical yield of liquid hydrocarbons after the complete hydrodeoxygenation of such oil must be 86.0%. The theoretical yield would be 81.0% if oxygen is removed only in the form of carbon oxides [15].

The yield and hydrocarbon composition of the products formed during hydrodeoxygenation depends on the content of zeolite in the support of the catalyst (Fig. 2). The yield of C$_{5+}$ hydrocarbons was 75−79%. It grew with experiment time, because the strongest catalyst acid sites, on which cracking reaction occur, were deactivated. An increase in the total acidity of catalysts as their content of zeolite grew reduced the yield of liquid products (see Table 1), because the contribution from reactions of cracking with the formation of C$_5$−C$_{14}$ hydrocarbons and C$_3$−C$_4$ gases also grew (see Fig. 2).

As noted above, the gases contain carbon monoxide and dioxide in addition to C$_1$−C$_4$ hydrocarbons. Molar ratios C$_3$H$_8$: CO$_2$: CO, calculated by analyzing gaseous products of the process, are given in Table 2. The selectivity of decarboxylation (deCO$_2$) for all samples was 14−22%, and the selectivity of decarbonylation (deCO) was 27−30%. The total selectivity toward decarboxylation and decarbonylation (deCO$_x$) reactions was slightly lower than the one calculated using ratio (C$_{15}$ + C$_{17}$)/ΣC$_{15-18}$ (Fig. 5b), especially for the samples with a high zeolite contents. However, the gaseous products were found to have a considerable content of methane, which can be formed during the hydrodeoxygenation of sunflower oil in the side CO and CO$_2$ methanation reactions [10] and the hydrogenolysis of C−C bonds in the glycerol residues of triglycerides with the formation of methane and ethane [20, 21]. We can see from the data of Table 2 that the molar ratio of propane to liquid hydrocarbons (C$_3$H$_8$: C$_{5+}$) was lower than that of glycerin to fatty acid residues in oils (0.33), and the ratio of the molar yields of C$_1$ compounds (methane, CO and CO$_2$) to the yield of hydrocarbons with an odd number of carbon atoms in their chains exceeds the stoichiometric value (1 : 1).
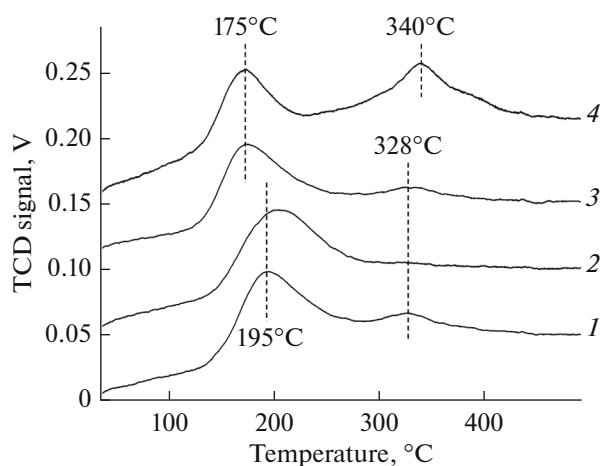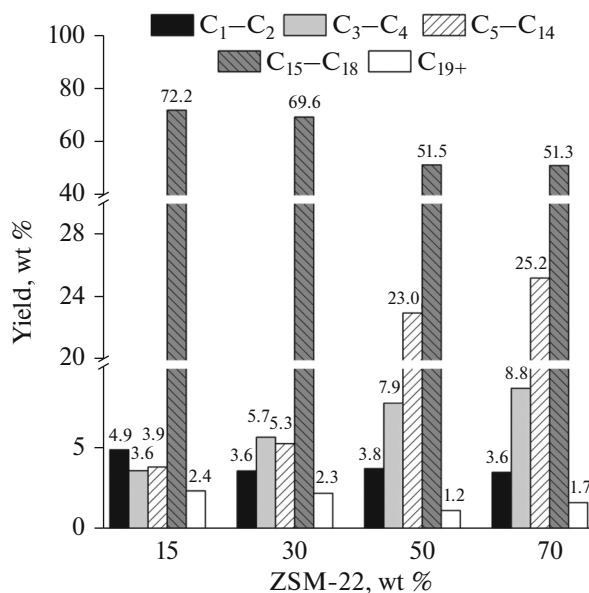
Fig. 3. TPR profiles of (*1*) 1% Pt/Z(15), (*2*) 1% Pt/Z(30), (*3*) 1% Pt/Z(50), and (*4*) 1% Pt/Z(70) catalysts. Unreduced samples synthesized by impregnating the prepared supports with H_2PtCl_6 further drying at 120°C and calcination at 450°C, were used in this work.

Fig. 4. Yield of hydrocarbon products of sunflower oil hydrodeoxygenation versus zeolite content in the catalyst support. Process conditions: temperature, 320°C; pressure, 4 MPa; WHSV = 1 h^{-1}; H_2 : feedstock = 2500 Nm^3/m^3; time, 4 h.

These results confirm the assumed scheme of triglyceride decomposition and the occurrence of side methanation reactions during the hydrodeoxygenation of sunflower oil on the studied catalysts.

The dependences measured for the content of *iso*-alkanes in C_{11}–C_{20} hydrocarbons (diesel fraction) when testing the series of 1% Pd/Z(*x*) catalysts in the hydrodeoxygenation of sunflower oil are shown in Fig. 5. We can see that at the initial time moment, the content of isomers grew along with the content of zeolite in the support from 36% (at a zeolite content of 15 wt %) to 72% (70 wt % of zeolite). However, the isomerizing ability of the catalysts fell by 1.5−2.5 times in 4 h independently of the zeolite content, due to the coking and deactivation of acid catalyst sites.

Since triglycerides of vegetable oils contain fatty acids exclusively with an even number of carbon atoms in their chains (C_{16} and C_{18}), the content of C_{15} and C_{17}

hydrocarbons in products can be used to estimate the contribution from decarbonylation and decarboxylation (deCO_x) reactions, relative to direct hydrodeoxygenation (HDO). When the zeolite content was raised from 15 to 70 wt %, the content of products resulting from deCO_x reactions fell to 66 and 53% (after 2h of the catalyst's operation).

Effect of the Temperature

It is known that temperature has a strong effect on the rates of deoxygenation and isomerization reactions [11, 22−24]. In this study, experiments with 1% Pt/Z(50) catalyst were performed to estimate the

Table 2. Composition of gaseous products of sunflower oil hydrodeoxygenation with catalysts 1% Pt/Z(*x*)*

Sample	$Y(CO + CO_2)$, wt%	$C_3H_8 : CO_2 : CO$	$(CO_2 + CO + CH_4) : C_{n-1}$**	$C_3H_8 : C_{5+}$
1% Pt/Z(15)	3.7	1 : 0.58 : 0.90	1.53	0.22
1% Pt/Z(30)	3.9	1 : 0.65 : 0.85	1.93	0.15
1% Pt/Z(50)	5.3	1 : 0.62 : 0.80	2.05	0.27
1% Pt/Z(70)	5.7	1 : 0.42 : 0.81	1.88	0.29

* Reaction conditions: temperature, 320°C; pressure, 4 MPa; WHSV = 1 h^{-1}; H_2 : feedstock = 2500 Nm^3/m^3; time, 4 h. Yield of products according to gas chromatography data.
** *n* is the number of C atoms in the initial carboxylic acid.
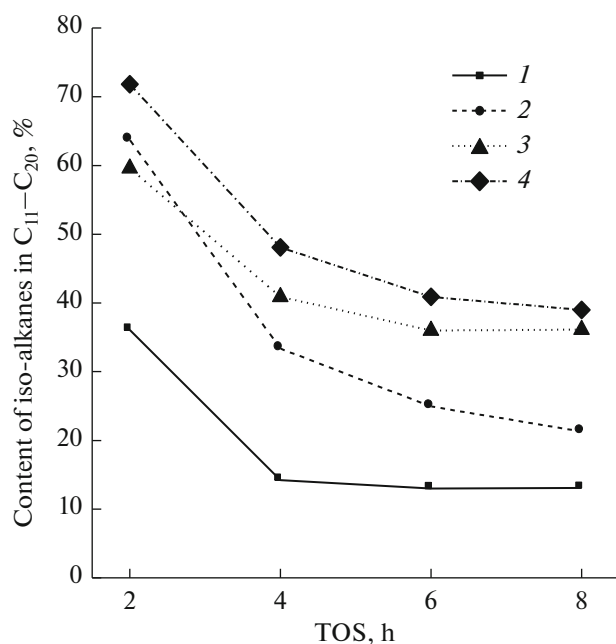
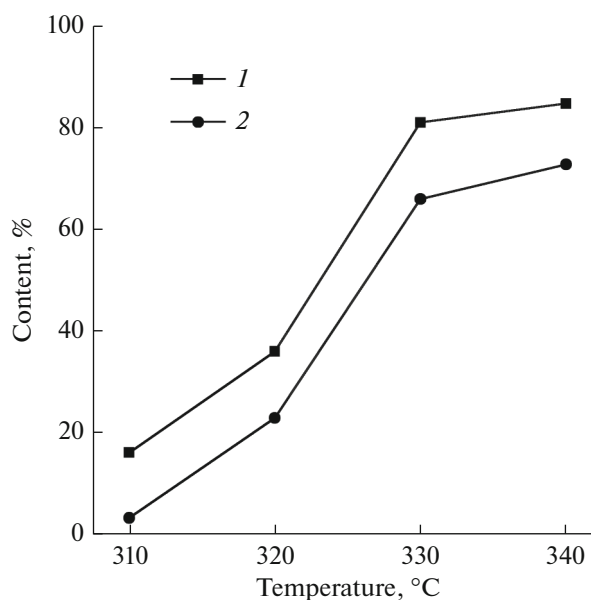**Fig. 5.** Content of *iso*-alkanes in $C_{11}-C_{20}$ hydrocarbons (diesel fraction) versus the time on stream for catalysts (*1*) 1% Pt/Z(15), (*2*) 1% Pt/Z(30), (*3*) 1% Pt/Z(50), and (*4*) 1% Pt/Z(70).

Fig. 6. Effect of the temperature on the content of (*1*) C_5-C_{14} hydrocarbons and (*2*) *iso*-alkanes in liquid products. Catalyst 1% Pt/Z(50); pressure, 4 MPa; WHSV = 1 h^{-1}; H_2 : feedstock = 2500 Nm^3/m^3.

effect of the temperature on the yield of. The temperature was varied from 310 to 340°C. No other parameters were changed: pressure, 4 MPa; WHSV = 1 h^{-1}; and H_2 : feedstock = 2500 Nm^3/m^3.

Analysis of liquid sunflower oil hydrodeoxygenation products in the above range of temperatures confirmed the absence of oxygen-containing compounds, testifying to the complete deoxygenation of the feedstock.

The alkanes formed at the stage of deoxygenation rearranged using intermediate carbenium compounds with the participation of metallic and acid catalyst sites. Once adsorbed on acid catalyst sites, the latter were subjected to reactions of isomerization and cracking. The rates of both reactions grew along with the temperature. As is shown in Fig. 6, the content of *iso*-alkanes in the diesel fraction ($C_{11}-C_{20}$ hydrocarbons) and products of the cracking reaction (C_5-C_{14} hydrocarbons) grew symbatically when the temperature was raised.

The relative content of C_{15} and C_{17} hydrocarbons in the products was 45%. When the temperature was raised to 320°C, it grew to 57%. Raising the temperature again lowered their content to 53% at 330°C and 41% at 340°C. The content of C_5-C_{14} hydrocarbons in the products rose from 3 to 73% after the temperature was increased to 340°C, making it impossible to estimate correctly the effect of the process temperature on

the paths of deoxygenation in the single-stage processing of sunflower oil.

An increase in the ratio $(CO_2 + CO + CH_4)/C_{n-1}$ from 1.2 to 11.7 along with temperature indicates the contribution from side reactions grew substantially. The relatively high yields obtained for propane (up to 17%) and butanes (up to 21%) at temperatures of 330 and 340°C also indicate the occurrence of intense hydrocracking reactions.

Effect of the Weight Hourly Space Velocity

To estimate the effect WHSV had on the yield and composition of products of sunflower oil hydrodeoxygenation, tests were performed in the WHSV range of 0.8 to 3 h^{-1} with all other conditions of the process remaining constant: temperature, 330°C; pressure, 4 MPa; and H_2 : feedstock = 2500 Nm^3/m^3. A sample of 1% Pt/Z(50) was used as the catalyst.

It was found that the feedstock was completely converted under the above conditions of hydrodeoxygenation at the selected WHSV values. At the same time, WHSV had a strong effect on reactions of cracking and methanation: the contribution from these reactions grew as WHSV fell and the content of C_5-C_{14} hydrocarbons and C_3-C_4 gases in the products rose (Fig. 7). The effect of WHSV on the content of *iso*-alkanes in the diesel fraction was similar. Cracking and isomerization reactions were therefore suppressed when the period of contact between the feedstock and the catalyst was shortened. However, ratio $(C_{15} + C_{17})/\Sigma C_{15-18}$ in the liquid product grew slightly along with WHSV,
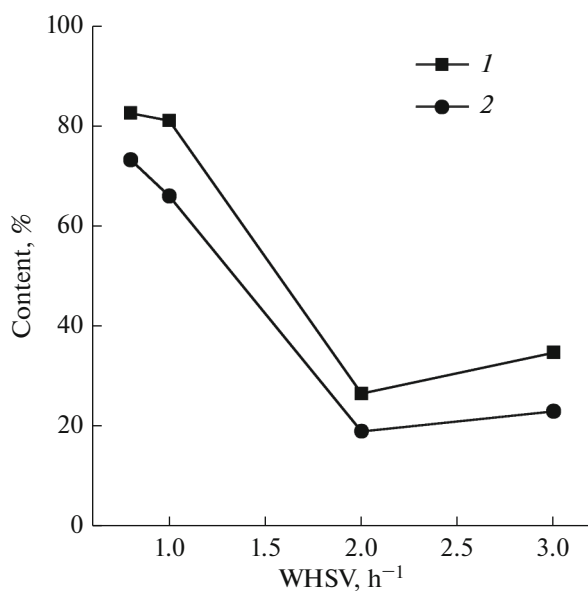
Fig. 7. Effect of WHSV on the content of (*1*) C_5-C_{14} hydrocarbons and (*2*) *iso*-alkanes in liquid products. Catalyst 1% Pt/Z(50); pressure, 4 MPa; temperature, 330°C; H_2 : feedstock = 2500 Nm^3/m^3.
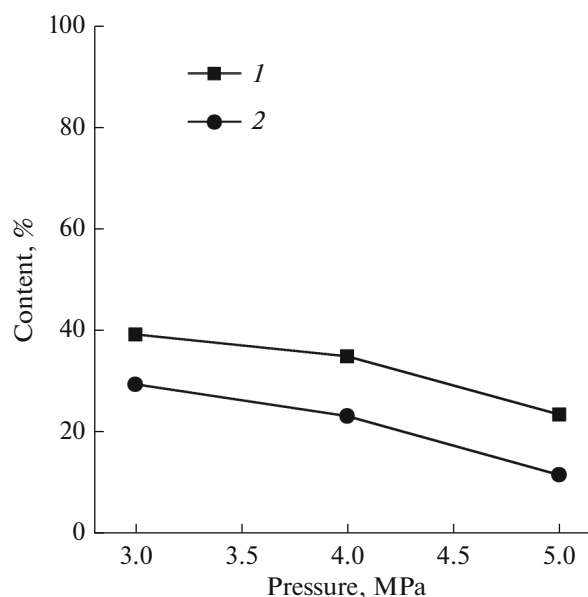
Fig. 8. Effect of the pressure on the content of (*1*) C_5-C_{14} hydrocarbons and (*2*) *iso*-alkanes in liquid products. Catalyst 1% Pt/Z(50); temperature, 330°C; WHSV = 1 h^{-1}; H_2 : feedstock = 2500 Nm^3/m^3.

indicating an increased contribution from reactions of $deCO_x$ relative to HDO when the time of contact was shortened. One reason for this could be a low rate of triglyceride hydrocracking with the formation of free fatty acids (which requires longer periods of contact between the reagent and the catalyst), relative to the rate of $-C(=O)-C_n$ bond cleavage [21].

The degree of hydrogenation (saturation) for the C=C bonds in triglycerides molecules is a parameter that can be used to judge the efficiency of the hydroprocessing of vegetable oils. The sunflower oil used in this study was 89.4% unsaturated acids (generally, olein and linoleic) [15]. It was established that WHSV had no appreciable effect on the saturation of double bonds, but some unsaturated and aromatic hydrocarbons were revealed in the liquid products of the reaction at WHSV values above 1 h^{-1}. These results indicate that the hydrogenation of unsaturated compounds is incomplete at short periods of contact.

Effect of the Pressure

Another important factor influencing the path of vegetable oil deoxygenation is the partial hydrogen pressure. To study the effect hydrogen of the on the yield and composition of products of sunflower oil hydrodeoxygenation, tests were performed at 3, 4, and 5 MPa. The other conditions of the process were kept constant: temperature, 330°C; WHSV = 1 h^{-1}, and H_2 : feedstock = 2500 Nm^3/m^3. A sample of 1% Pt/Z(50) was used as a catalyst.

It was established that the feedstock was fully converted under the above conditions of hydrodeoxygenation at all selected hydrogen pressures. At the same time, the pressure affected the yield of products. When it was raised from 3 to 5 MPa, the content of C_5-C_{14} hydrocarbons in the liquid products fell from 39 to 24% (Fig. 8), and the total yield of C_{5+} hydrocarbons did not change appreciably ($\approx$83%). This indicates that raising the pressure reduces the contribution from cracking reactions.

We can see from Fig. 8 that the content of *iso*-alkanes in the diesel fraction fell from 30 to 12% when the pressure was raised from 3 to 5 MPa. A possible reason is the blocking of active catalyst sites by hydrogen molecules upon raising its partial pressure.

At the same time, a high partial hydrogen pressure promotes HDO reactions, so the content of hydrocarbons with an odd number of carbon atoms in their chains fell from 72 to 64%. These results agree with the data in [22–25].

CONCLUSIONS

(1) The effect of the ZSM-22 content in the support on the yield and composition of sunflower oil hydrodeoxygenation products was studied for the 1%Pt/Al_2O_3–ZSM-22 catalyst and process parameters (temperature, pressure, and WHSV). Complete hydrodeoxygenation was observed for the feedstock throughout the range of process conditions. At a temperature of 320°C, a pressure of 4 MPa, and WHSV =

1 h^{-1}, the yield of C$_{5+}$ hydrocarbons was 75−79% and grew along with the duration of the experiment.

(2) It was established that the content of strong acid sites in the catalyst grows when the zeolite content in its support is raised from 15 to 70% to accelerate cracking reactions with the formation of C$_5$−C$_{14}$ hydrocarbons and C$_3$−C$_4$ gases and raise the content of *iso*-alkanes in the liquid products from 36 to 72%. However, the process selectivity toward *iso*-alkanes falls by 1.5−2.5 times over 4 h due to deactivation of the catalyst, independently of the zeolite content.

(3) An rise in temperature or a drop in pressure during the process promotes decarboxylation/decarbonylation reactions and intensify cracking and isomerization reactions.

(4) Complete hydrodeoxygenation was observed for sunflower oil in the WHSV range of 2−3 h^{-1}. The content of cracking products in liquid hydrocarbons was less than 30 wt % (for a sample with a 50% content of zeolite in its support), and the content of *iso*-paraffins was no more than 20 wt %. Reducing WHSV to 0.5−1 h^{-1} allows us to obtain hydrocarbon products that are up to 70% *iso*-alkanes, but the content of cracking products can reach 80% under such conditions.

CONFLICT OF INTEREST

The authors declare that they have no conflict of interests.

REFERENCES

1. Huber, G.W., Iborra, S., and Corma, A., *Chem. Rev.,* 2006, vol. 106, no. 9, pp. 4044−4098.
https://doi.org/10.1021/cr068360d

2. Sivasamy, A., Cheah, K.Y., Fornasiero, P., Kemausuor, F., Zinoviev, S., and Miertus, S., *ChemSusChem,* 2009, vol. 2, no. 4, pp. 278−300.
https://doi.org/10.1002/cssc.200800253

3. Choudhary, T.V. and Phillips, C.B., *Appl. Catal., A,* 2011, vol. 397, nos. 1−2, pp. 1−12.
https://doi.org/10.1016/j.apcata.2011.02.025

4. Khan, S., Kay Lup, A.N., Queshi, K.M., Abnisa, F., Wan Daud, W.M.A., Patah, M.F.A., *Anal. Appl. Pyrolysis,* 2019, vol. 140, pp. 1−24.
https://doi.org/10.1016/j.jaap.2019.03.005

5. Douvartzides, S.L., Charisiou, N.D., Papageridis, K.N., and Goula, M.A., *Energies,* 2019, vol. 12, no. 5, article no. 809.
https://doi.org/10.3390/en12050809

6. Smirnova, M.Yu., Kikhtyanin, O.V., Rubanov, A.E., Trusov, L.I., and Echevskii, G.V., *Catal. Ind.,* 2013, vol. 5, no. 3, pp. 253−259.
https://doi.org/10.1134/S2070050413030112

7. Pérez-Cisneros, E.S., Sales-Cruz, M., Lobo-Oehmichen, R., and Viveros-García, T., *Comput. Chem. Eng.,* 2017, vol. 105, pp. 105−122.
https://doi.org/10.1016/j.compchemeng.2017.01.018

8. Herskowitz, M., Landau, M.V., Reizner, Y., and Berger, D., *Fuel,* 2013, vol. 111, pp. 157−164.
https://doi.org/10.1016/j.fuel.2013.04.044

9. Wang, C., Liu, Q., Liu, X., Yan, L., Luo, C., Wang, L., Wang, B., and Tian, Z., *Chin. J. Catal.,* 2013, vol. 34, no. 6, pp. 1128−1138.
https://doi.org/10.1016/S1872-2067(11)60524-X

10. Wang, C., Tian, Z., Wang, L., Xu, R., Liu, Q., Qu, W., Ma, H., and Wang, B., *ChemSusChem,* 2012, vol. 5, no. 10, pp. 1974−1983.
https://doi.org/10.1002/cssc.201200219

11. Wang, C., Liu, Q., Song, J., Li, W., Li, P., Xu, R., Ma, H., and Tian, Z., *Catal. Today,* 2014, vol. 234, pp. 153−160.
https://doi.org/10.1016/j.cattod.2014.02.011

12. Zhang, M., Chen, Y., Wang, L., Zhang, Q., Tsang, C.-W., and Liang, C., *Ind. Eng. Chem. Res.,* 2016, vol. 55, no. 21, pp. 6069−6078.
https://doi.org/10.1021/acs.iecr.6b01163

13. Martens, J.A., Verboekend, D., Thomas, K., Vanbutsele, G., Pérez-Ramírez, J., and Gilson, J.-P., *Catal. Today,* 2013, vols. 218−219, pp. 135−142.
https://doi.org/10.1016/j.cattod.2013.03.041

14. Hancsók, J., Krár, M., Magyar, S., Boda, L., Holló, A., and Kalló, D., *Microporous Mesoporous Mater.,* 2007, vol. 101, nos. 1−2, pp. 148−152.
https://doi.org/10.1016/j.micromeso.2006.12.012

15. Nepomnyashchiy, A.A., Buluchevskiy, E.A., Lavrenov, A.V., Yurpalov, V.L., Gulyaeva, T.I., Leont'eva, N.N., and Talzi, V.P., *Russ. J. Appl. Chem.,* 2017, vol. 90, no. 12, pp. 1944−1952.
https://doi.org/10.1134/S1070427217120084

16. Parmar, S., Pant, K.K., John, M., Kumar, K., Pai, S.M., and Newalkar, B.L., *Energy Fuels,* 2015, vol. 29, no. 2, pp. 1066−1075.
https://doi.org/10.1021/ef502591q

17. Chi, K., Zhao, Z., Tian, Z., Hu, S., Yan, L., Li, T., Wang, B., Meng, X., Gao, S., Tan, M., and Liu, Y., *Pet.*

Sci., 2013, vol. 10, no. 2, pp. 242−250.
https://doi.org/10.1007/s12182-013-0273-6

18. Liu, S., Ren, J., Zhu, S., Zhang, H., Lv, E., Xu, J., and Li, Y.-W., *J. Catal.,* 2015, vol. 330, pp. 485−496.
https://doi.org/10.1016/j.jcat.2015.07.027

19. Liu, S., Ren, J., Zhang, H., Lv, E., Yang, Y., and Li, Y.-W., *J. Catal.,* 2016, vol. 335, pp. 11−23.
https://doi.org/10.1016/j.jcat.2015.12.009

20. Kim, S.K., Han, J.Y., Lee, H.S., Yum, T., Kim, Y., and Kim, J., *Appl. Energy,* 2014, vol. 116, pp. 199−205.
https://doi.org/10.1016/j.apenergy.2013.11.062

21. Alcalá, R., Mavrikakis, M., and Dumesic, J.A., *J. Catal.,* 2003, vol. 218, no. 1, pp. 178−190.
https://doi.org/10.1016/S0021-9517(03)00090-3

22. Chen, N., Gong, S., Shirai, H., Watanabe, T., and Qian, E.W., *Appl. Catal., A,* 2013, vol. 466, pp. 105−115.
https://doi.org/10.1016/j.apcata.2013.06.034

23. Sankaranarayanan, T.M., Banu, M., Pandurangan, A., and Sivasanker, S., *Bioresour. Technol.,* 2011, vol. 102, no. 22, pp. 10717−10723.
https://doi.org/10.1016/j.biortech.2011.08.127

24. Anand, M. and Sinha, A.K., *Bioresour. Technol.,* 2012, vol. 126, pp. 148−155.
https://doi.org/10.1016/j.biortech.2012.08.105

25. Guzman, A., Torres, J.E., Prada, L.P., and Nuñez, M.L., *Catal. Today,* 2010, vol. 156, nos. 1−2, pp. 38−43.
https://doi.org/10.1016/j.cattod.2009.11.015

Translated by E. Glushachenkova

Publisher's Note. Pleiades Publishing remains neutral with regard to jurisdictional claims in published maps and institutional affiliations.